of pressure, the other axis ($a_0$) contracts.

It may be observed from Tables I and II that an anion effect on the "d–d" transitions exists as pressures are increased. A decrease in the high-energy shifts (blue) with pressure occurs. The more polarizable or softer[11] anions show a smaller blue shift. Results are similar to those obtained for $Et_2en$,[8] although of smaller magnitude.

## Experimental Section

**Preparation.** The amine ligands *N,N*-$Me_2en$ and *C,C*-$Me_2en$ were commercially obtained (Fluka) and were purified by distillation. The complexes were prepared according to procedure by Goodgame and Venanzi.[12] The complexes containing halometalates as anions were obtained by the method of Fabbrizzi et al.[7] Analyses gave satisfactory results.

**Spectral Measurements.** Electronic spectra under high external pressure were obtained in a diamond anvil cell[13] using a Cary 14 spectrophotometer interfaced with a special beam condenser.[14] The spectra at elevated temperatures were recorded with a Beckman DK-2A spectrophotometer. The complexes were spread on a filter paper and maintained in a thermostated cell. The temperature was controlled by a calibrated thermistor.

**Registry No.** Ni(*C,C*-$Me_2en)_2(BF_4)_2$, 62682-83-1; Ni(*C,C*-$Me_2en)_2(NO_3)_2$, 62682-85-3; Ni(*C,C*-$Me_2en)_2(ClO)_2$, 62682-84-2; Ni(*C,C*-$Me_2en)_2Br_2$, 19502-59-1; Ni(*C,C*-$Me_2en)_2I_2$, 19502-60-4; Ni(*C,C*-$Me_2en)_2CdBr_4$, 62669-54-9; Ni(*C,C*-$Me_2en)_2(AgI_2)_2$, 62669-53-8; Cu(*C,C*-$Me_2en)_2(NO_3)_2$, 62669-52-7; Ni(*N,N*-$Me_2en)_2(BF_4)_2$, 62669-55-0; Ni(*N,N*-$Me_2en)_2(ClO_4)_2$, 55326-15-3; Ni(*N,N*-$Me_2en)_2CdBr_4$, 62669-57-2; Ni(*N,N*-$Me_2en)_2HgI_4$, 62669-58-3; Ni(*N,N*-$Me_2en)_2I_2$, 62669-56-1.

## References and Notes

(1) Based on work performed under the auspices of the Division of Physical Research of the U.S. Energy Research and Development Administration.
(2) Universita di Firenze, II Cattedra di Chemica Generale ed Inorganica, Firenze, Italy.
(3) D. M. L. Goodgame and L. M. Venanzi, *J. Chem. Soc.*, 616 (1963).
(4) W. E. Hatfield, T. S. Piper, and U. Klabunde, *Inorg. Chem.*, **2**, 629 (1963).
(5) A. B. P. Lever, E. Montovani, and J. C. Domini, *Inorg. Chem.*, **10**, 2424 (1971).
(6) B. P. Kennedy and A. B. P. Lever, *J. Am. Chem. Soc.*, **95**, 6907 (1973).
(7) L. Fabbrizzi, M. Micheloni, and P. Paoletti, *Inorg. Chem.*, **13**, 3019 (1974).
(8) J. R. Ferraro, L. J. Basile, L. R. Garcia-Ineguez, P. Paoletti, and L. Fabbrizzi, *Inorg. Chem.*, **15**, 2342 (1976).
(9) H. G. Drickamer, R. W. Lynch, R. L. Clendenen, and E. A. Perez-Albuerne, *Festkoerperprobleme*, **19**, 135 (1966).
(10) J. R. Ferraro, *J. Chem. Phys.*, **53**, 117 (1970).
(11) R. G. Pearson, *J. Am. Chem. Soc.*, **85**, 3533 (1963).
(12) D. M. L. Goodgame and L. M. Venanzi, *J. Chem. Soc.*, 5909 (1963).
(13) J. R. Ferraro and L. J. Basile, *Appl. Spectrosc.*, **28**, 505 (1974).
(14) G. J. Long, Miles, and J. R. Ferraro, *Appl. Spectrosc.*, **28**, 3776 (1974).

---

Contribution from the Chemistry Division,
Argonne National Laboratory, Argonne, Illinois 60439

# Structural Studies of Precursor and Partially Oxidized Conducting Salts. 12. Crystal Structure of $Rb_2[Pt(CN)_4](FHF)_{0.40}$. A New Lower Limit for the Platinum–Platinum Separation and the First Anhydrous One-Dimensional Tetracyanoplatinate Complex[1]

Arthur J. Schultz,[2a] Christopher C. Coffey,[2b] Grace C. Lee,[2c] and Jack M. Williams*

*Received February 25, 1977* AIC701499

It has been postulated[3,4] that the Peierls transition from a metallic to a low-temperature insulating state in one-dimensional conductors can be suppressed by increasing the interchain coupling. One method for testing these theoretical predictions involves the preparation of a series of similar materials in which the one-dimensional properties are preserved and the effects of various modifications can be investigated.

**Table I**

Positional and Thermal Parameters for $Rb_2[Pt(CN)_4](FHF)_{0.40}$

| Atom | $x^a$ | $y$ | $z$ | $B$,$^b$ Å$^2$ |
|---|---|---|---|---|
| Pt | 0.0 | 0.0 | 0.0 | *c* |
| C | 0.0550 (8) | 0.1480 (8) | 0.0 | *c* |
| N | 0.0871 (8) | 0.2325 (8) | 0.0 | *c* |
| Rb | 0.1555 (3) | 0.6555 | 0.0 | *c* |
| F(1) | 0.0 | 0.5 | 0.155 (14) | 4.9 (11) |
| F(2) | 0.0 | 0.5 | 0.25 | 5.7 (13) |

Anisotropic Thermal Parameters ($\times 10^4$)$^d$

| Atom | $\beta_{11}$ | $\beta_{22}$ | $\beta_{33}$ | $\beta_{12}$ | $\beta_{13}$ | $\beta_{23}$ |
|---|---|---|---|---|---|---|
| Pt | 25.3 (5) | 25.3 | 84 (2) | 0 | 0 | 0 |
| C | 48 (7) | 27 (5) | 117 (29) | 1 (5) | 0 | 0 |
| N | 59 (7) | 51 (7) | 295 (40) | −15 (6) | 0 | 0 |
| Rb | 72 (2) | 72 | 382 (8) | 27 (1) | 0 | 0 |

$^a$ $x$, $y$, and $z$ are fractional coordinates. $^b$ Isotropic temperature factor of the form $\exp(-B^2(\sin^2\theta)/\lambda^2)$. $^c$ Atoms refined anisotropically. $^d$ Anisotropic thermal parameters of the form $\exp[-(h^2\beta_{11} + k^2\beta_{22} + l^2\beta_{33} + 2hk\beta_{12} + 2hl\beta_{13} + 2kl\beta_{23})]$.

This has been successful to some extent in the study of TTF–TCNQ and its many analogues.[5a] However, numerous attempts to prepare partially oxidized tetracyanoplatinate (POTCP) complexes,[5] of which $K_2[Pt(CN)_4]X_{0.3}\cdot 3H_2O$, X = Cl or Br, "KCP(X)", is the prototype, with anions other than $Cl^-$ or $Br^-$ have been unsuccessful. This is the case even for the simplest derivatives such as $F^-$ or $I^-$.

In order to both prepare a new KCP(X) type derivative and, at the same time, increase interchain coupling (hopefully) through H-bonding interactions, we have synthesized an entirely new series of POTCP salts containing the triatomic bifluoride $(FHF)^-$ ion. These salts are most extraordinary and in this communication we wish to report the improved synthesis and the crystal structure of $Rb_2[Pt(CN)_4](FHF)_{0.40}$, RbCP(FHF), which has the shortest Pt–Pt distance (2.798 (1) Å) yet observed for any POTCP complex.

The preparation of RbCP(FHF) herein is slightly modified from that previously reported.[6] Needle-shaped crystals up to 5 mm in length were grown electrolytically from a 6 mL solution of 1.08 g of $Rb_2[Pt(CN)_4]\cdot 1.5H_2O$ to which 3 mL of concentrated HF and 2.0 g of RbF were added. The solution was electrolyzed at 1.5 V in a polyethylene beaker with Pt electrodes over a period of 24 h. The lustrous metallic gold-colored crystals were washed with cold water, and elemental analysis[7] indicated the formula to be $Rb_2[Pt(CN)_4](FHF)_{0.40}$ for the new material.

A 0.34 mm long crystal was cut (0.0036 mm$^2$ cross section) and was used for data collection on a Syntex $P2_1$ diffractometer equipped with a graphite monochromator. Intensity measurements were made in the $\theta$–$2\theta$ step-scan mode using Mo K$\alpha$ x radiation. Weissenberg photographs of the RbCP(FHF) crystals exhibited body-centered tetragonal $4/mmm$ Laue symmetry ($h + k + l = 2n$) with the additional systematic absences $l = 2n + 1$ for the $h0l$ and $0kl$ reflections. The centrosymmetric space group $I4/mcm$ ($D_{4h}^{18}$, No. 140) was chosen initially and was justified by the satisfactory least-squares refinement ultimately obtained. The refined cell parameters (12 diffractometer-centered reflections) are $a$ = 12.689 (2) Å, $c$ = 5.595 (1) Å, and $V$ = 900.9 Å$^3$ with $Z$ = 4 and a calculated density of 3.58 g/cm$^3$. The structure was solved by a combination of direct methods, least-squares, and Fourier synthesis procedures to yield final agreement factors of $R(F_o) = 0.045$, $R(F_o^2) = 0.053$, and $R_w(F_o^2) = 0.070$ based on 383 independent reflections corrected for absorption ($\mu$ = 278.66 cm$^{-1}$). The final positional and thermal parameters are presented in Table I.

The crystal structure, as shown in Figure 1, consists of columnar chains of square-planar $Pt(CN)_4^{-1.60}$ groups which

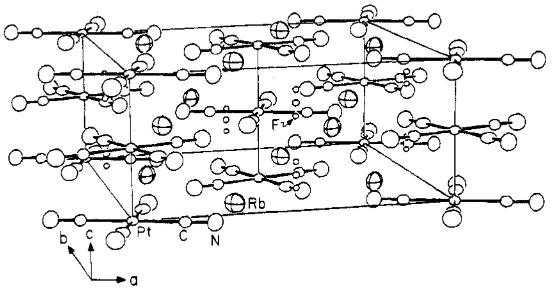

**Figure 1.** Perspective view of the unit cell of $Rb_2[Pt(CN)_4](FHF)_{0.40}$. The small circles are the partially occupied fluorine positions. The thermal ellipsoids of the other atoms are drawn with a scale of 50% probability.

stack parallel to *c*. The derived Pt–Pt distance (*c*/2) of 2.798 (1) Å is the shortest of any POTCP salt and is very close to the 2.77 Å internuclear separation in Pt metal itself. Crystallographic requirements are such that all Pt–Pt distances are equivalent, and the TCP moiety is constrained to be perfectly planar. In KCP(Br) and KCP(Cl) the Pt–Pt separations are equal at 2.88 ± 0.01 Å but are not constrained crystallographically to be equivalent. Neighboring TCP groups in RbCP(FHF) form a staggered configuration with a 49.2 (6)° torsion angle. The intramolecular bond lengths and angles are Pt–C = 2.00 (1) Å, C–N = 1.15 (1) Å, and Pt–C–N = 180 (1)°.

The presumed linear bifluoride anions $(FHF)^-$ are aligned parallel to *c* and symmetry related sites (see Figure 2) generate a F(1)···F(2) distance of 2.27 (8) Å. This is in good agreement with F···F distances found in simple alkali metal bifluoride salts.[8] Each fluorine site is only partially occupied and therefore the $(F-H-F)^-$ group is disordered. A schematic representation of the possible positions and orientations of the $(F-H-F)^-$ anions is shown in Figure 2. It is crystallographically possible to have a $(FHF)^-$:Pt ratio as high as 0.5:1 when short F···F contacts are prohibited. Refinement of the fluorine multipliers leads to 0.41 ± 0.02 bifluoride anions, which agrees well with the analytical data.

We previously proposed[6] the existence of at least one water of hydration per molecular formula. However, no evidence of a water site in the crystal structure was observable from the x-ray data. Furthermore, thermal gravimetric analysis of RbCP(FHF) and the Cs analogue, $Cs_2[Pt(CN)_4](FHF)_{0.39}$, shows no evidence for the presence of water. We therefore believe that these two materials are the first known POTCP complexes which are completely anhydrous, although final verification of this will have to await a neutron diffraction analysis. It has been noted[9] that the physical properties of KCP(Cl,Br) are influenced by the dependence of their degrees of hydration on atmospheric and temperature conditions. This lack of stability should not be a problem with CsCP(FHF) and RbCP(FHF). The absence of interchain hydrogen bonding as a means for crystal stabilization indicates that the binding forces must be due to stronger Coulombic $[Rb^+\cdots X^-]$ interactions alone. In RbCP(FHF), all rubidium cations occupy sites in the same plane as the $Pt(CN)_4^{-1.60}$ groups, such that there are four short Rb···N contacts of 3.26 Å out of the plane and two each of 3.39 and 3.41 Å within the $Pt(CN)_4$ plane. The closest Rb···F contacts are 2.92, 3.12, and 3.39 Å which may be compared with Rb···F distances of 2.27 Å in the gas phase and 2.84 Å in crystalline RbF.

As predicted from Pauling's theory of metals,[10-12] along with the shortest known POTCP salt Pt–Pt distance, RbCP(FHF) has the highest degree of partial oxidation (although CsCP(FHF) may share this honor) of any known TCP complex. Using the equation[10] $D(n) = D(1) - 0.600 \log n$, where $D(n)$ is the metal–metal distance with bond order $n$ and $D(1)$ is the single bond length (2.59 Å for Pt), $D(n) = 2.83$ Å with $n = 0.40$ or, conversely, $n = 0.45$ with $D(n) = 2.80$ Å. Although this is not in good agreement with the experimental values, the general trend for the POTCP salts[11,12] is still qualitatively observed. Furthermore, it now appears that, as expected, shorter Pt–Pt separations (higher degree of partial oxidation) result in higher conductivity. Our preliminary four-probe conductivity measurements at room temperature indicate the conductivity of CsCP(FHF) is at least two times greater than that of KCP(Cl). Therefore, if the trend of conductivities CsCP(FHF) > KCP(Cl) > K(def)TCP[13] continues to be inversely related to the Pt–Pt separations (2.83, 2.87, and 2.96 Å, respectively), RbCP(FHF), with Pt–Pt = 2.80 Å, should have the highest conductivity of the known POTCP complexes. Furthermore, in RbCP(FHF) the interchain Pt–Pt separation is 8.98 Å as compared to 9.91 Å in KCP(Br). It is possible that this shorter interchain distance may increase interchain coupling and result in suppression of the Peierls transition to a lower temperature. Measurements of the electrical conductivity, plasma edge frequency, and possible superlattice (diffuse x-ray scattering) are underway to further characterize the properties of RbCP(FHF).

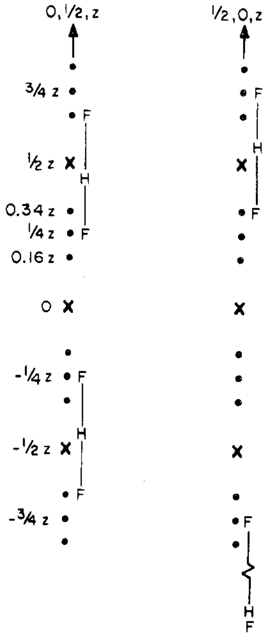

**Figure 2.** Schematic representation of the possible positions and orientations of $(F-H-F)^-$ anions along two parallel chains. The positions of the hydrogen atoms have not been located from the x-ray data. Therefore, the linearity of the $(F-H-F)^-$ ion or the symmetrical location of H between F atoms has not been experimentally determined. The dots represent all partially occupied *F* sites while the crosses only indicate the coordinates where $z = 0$ and $\pm 1/2$.

**Registry No.** $Rb_2[Pt(CN)_4]$, 15321-31-0.

**Supplementary Material Available:** A listing of structure factor amplitudes for $Rb_2[Pt(CN)_4](FHF)_{0.40}$ (3 pages). Ordering information is given on any current masthead page.

## References and Notes

(1) Work performed under the auspices of the Division of Physical Research of the U.S. Energy Research and Development Administration.
(2) (a) Support provided by the National Science Foundation under Grant No. CHE-76-07409. Undergraduate research participants sponsored by the Argonne Center for Educational Affairs from (b) Mercyhurst College, Erie, Pa., and (c) St. Mary of the Woods College, St. Mary of the Woods, Ind.
(3) M. Thielemans, R. Deltour, D. Jerome, and J. R. Cooper, *Solid State Commun.*, **19**, 21 (1976).
(4) B. Horovitz and A. Birnboim, *Solid State Commun.*, **19**, 91 (1976).
(5) For reviews, see (a) G. D. Stucky, A. J. Schultz, and J. M. Williams, *Annu. Rev. Mater. Sci.*, **7**, 301 (1977); (b) J. S. Miller and A. J. Epstein, *Prog. Inorg. Chem.*, **20**, 1 (1976).
(6) J. M. Williams, D. G. Gerrity, and A. J. Schultz, *J. Am. Chem. Soc.*, **99**, 1668 (1977).

(7) Elemental analyses performed by Midwest Microlabs. Anal. Calcd for $Rb_2[Pt(CN)_4](FHF)_{0.40}$: C, 9.89; N, 11.54; H, 0.08; F, 3.13. Found: C, 9.66; N, 10.53; H, 0.15; F, 3.05, 3.15. Emission spectrographic analyses for metal content performed by J. P. Faris indicated only Rb and Pt were present.

(8) H. L. Carell and J. Donohue, *Isr. J. Chem.*, **10**, 195 (1972).

(9) D. Cahen, *Solid State Commun.*, **12**, 1091 (1973).

(10) L. Pauling, "The Nature of the Chemical Bond", 3rd ed, Cornell University Press, Ithaca, N.Y., 1960, pp 398–404.

(11) J. M. Williams, *Inorg. Nucl. Chem. Lett.*, **12**, 651 (1976).

(12) A. H. Reis, Jr., and S. W. Peterson, *Inorg. Chem.*, **15**, 3186 (1976).

(13) T. W. Thomas, C. Hsu, M. M. Labes, P. S. Gomm, A. E. Underhill, and D. M. Watkins, *J. Chem. Soc., Dalton Trans.*, 2050 (1972); C. Jacobsen, K. Carneiro, and J. M. Williams, work in progress.

Contribution from the Instituto de Optica "Daza de Valdés",
C.S.I.C., Serrano, 121 Madrid-6, Spain

## A Model for B Carbonate Apatite

M. Santos* and P. F. González-Díaz

*Received January 26, 1977* AIC700695

Although the mechanism of substitution of $CO_3^{2-}$ ions and the precise site these ions occupy in the lattice of A carbonate apatite are well established,[1] neither a complete mechanism of $CO_3^{2-}$ substitution nor the exact site these ions occupy in the lattice of B carbonate apatite has hitherto been determined.[2] Nevertheless, it is known[3] that the *c* axis of the unit cell of B carbonate apatite and the perpendicular to the $CO_3^{2-}$ plane form an angle of around 35°.

Bonel et al.[4] have determined the $Ca^{2+}/PO_4^{3-}$, $Ca^{2+}/CO_3^{2-}$, and $Ca^{2+}/OH^-$ ratios in a great number of synthetic B carbonate apatites and proposed the general formula to account for these compounds

$$Ca_{10-x+u}(PO_4)_{6-x}(CO_3)_x(OH)_{2-x+2u}(H_2O)_z$$

**1**

where $0 \le x \le 2$, $0 \le u \le x/2$, and *z* is an unlimited variable. Since the substitution of a $PO_4^{3-}$ ion by a $CO_3^{2-}$ ion should leave a negative residual electric charge in the unit cell, Bonel et al. assumed that a couple, $OH^-$ and $Ca^{2+}$, is removed away from the apatitic lattice in each $PO_4^{3-}$–$CO_3^{2-}$ interchange, so that the number of $Ca^{2+}$ and $OH^-$ per unit cell decreases when substitution increases. Further, the *u* and *z* parameters in formula **1** are introduced to account only for the experimental values of the $Ca^{2+}/PO_4^{3-}$, $Ca^{2+}/CO_3^{2-}$, and $Ca^{2+}/OH^-$ ratios.

### Experimental Section

Stoichiometric and nonstoichiometric hydroxylapatite were prepared by a modified method of Winand.[5] A–B carbonate apatite was synthesized by a similar procedure in which sodium carbonate was added to the initial solution of $Na_2HPO_4$. B carbonate apatite was obtained by heating at 900 °C for 1 h a mixture of A–B carbonate apatite with calcium fluoride in a current of 2 cm³/s of dry $CO_2$. This reaction was carried out in a tube inserted in a furnace.

Biological carbonate apatites were provided by Dr. L. Cifuentes of the Urolithiasis Laboratory, Fundacion Jimenez Diaz, Madrid.

The x-ray diffraction pattern, electron microscopy, and electron diffraction diagram do not detect the presence of specimens such as $CaCO_3$, $CaHPO_4$, etc. in all of the samples so that these are practically constituted by single-phased nonstoichiometric carbonate apatites.

Infrared absorption spectra were recorded on a Perkin-Elmer 457 spectrophotometer in the range 4000–250 cm⁻¹. Absorption cells were prepared using the KBr disk technique.

### Results and Discussions

Figure 1 shows the mid-IR spectrum of a synthetic A–B carbonate apatite. $CO_3^{2-}$ bands in this spectrum appear at 1542, 1462, 1412, 880, and 872 cm⁻¹, which indicates that the two types of substitution (A and B) are present in this compound.

Figure 2 shows the mid-IR spectrum of the above sample heated at 900 °C for 3 h. In this spectrum, nearly stoichiometric hydroxylapatite $Ca_{10}(PO_4)_6(OH)_2$[5] and calcium hydroxide are seen; it can also be observed that some amount of the $CO_3^{2-}$ ions still remain inside the apatitic structure.

Since in the present conditions calcium hydroxide can only originate from calcium carbonate, it is not possible to postulate a general thermal mechanism by which formula **1** gives rise to the compound appearing in the IR spectrum of Figure 2. Moreover, as evidenced by this spectrum, the amount of $CO_3^{2-}$ ions included in the apatitic lattice is very small after calcination; therefore, some proportion of the stoichiometric hydroxylapatite observed in the spectrum of Figure 2 has to originate from the initial B carbonate apatite. This fact also cannot be explained by the formula assumed by Bonel et al.

Figure 3 reports the mid-IR spectrum of a B carbonate apatite. The $CO_3^{2-}$ IR bands appear at 1450, 1425, and 862 cm⁻¹. Figure 4 gives the mid-IR spectrum of the same sample after calcination at 900 °C. Besides the presence of some small proportion of $CO_3^{2-}$ ions included in the apatitic lattice, this spectrum corresponds to that of fluoroapatite, which confirms the above assessments.

A–B carbonate apatite might be obtained by $CO_3^{2-}$ diffusion through a suspension of nonstoichiometric hydroxylapatite.[6] However no carbonate apatite of any kind is formed in this process when stoichiometric hydroxylapatite is used.

Nonstoichiometric hydroxylapatite, $Ca_{10-x}(PO_4)_{6-x}(HPO_4)_x(OH)_{2-x}\cdot xH_2O$, differs from stoichiometric hydroxylapatite by possessing certain proportions of $HPO_4^{2-}$ ions and water molecules. Therefore, $HPO_4^{2-}$ ions and/or water molecules have to be responsible for the formation of carbonate apatites.

If we assume that $CO_3^{2-}$ ions substitute for $HPO_4^{2-}$ ions in nonstoichiometric hydroxylapatite, as the preceding synthetic procedure seems to indicate, the resulting compound would be electrically compensated.

$$Ca_{10-x}(PO_4)_{6-x}(CO_3)_x(OH)_{2-x}\cdot xH_2O$$

**2**

We have considered that the substitution of $HPO_4^{2-}$ by $CO_3^{2-}$ is complete. This does not modify the qualitative meaning of the arguments that hereafter will be presented.

Rotation of water molecules around the *c* axis in the unit cell of nonstoichiometric hydroxylapatite gives rise[7] to the alternative formation of the [$2PO_4^{3-}$, $OH^-$, $HPO_4^{2-}$] and [$3PO_4^{3-}$, $H_2O$] grouping through internal hydrogen migrations. When averaged over all possible water rotations in the crystal, the number of $HPO_4^{2-}$ ions and water molecules become the same in a dynamical equilibrium. Such an equilibrium is broken in formula **2**, so that the internal system, $H_2O$, $OH^-$, $PO_4^{3-}$, of the hypothetical compound represented by formula **2** has to evolve in order to recover the dynamical equilibrium between the $HPO_4^{2-}$ ions and the water molecules. Thus, formula **2** becomes

$$Ca_{10-x}(PO_4)_{6-3x/2}(CO_3)_x(HPO_4)_{x/2}(OH)_{2-x/2}\cdot(x/2)H_2O$$

**3**

Then, since the compound given by formula **3** has $HPO_4^{2-}$ ions, new substitutions may occur, giving

$$Ca_{10-x}(PO_4)_{6-3x/2}(CO_3)_{3x/2}(OH)_{2-x/2}\cdot(x/2)H_2O$$

**4**

where we have again assumed that all $HPO_4^{2-}$ have been substituted for by $CO_3^{2-}$ ions. Considerations made on formula **2** apply again to formula **4**; therefore, new $HPO_4^{2-}$ ions will be formed from water molecules. However these new $HPO_4^{2-}$ ions cannot now be substituted for by $CO_3^{2-}$ ions. In fact, $CO_3^{2-}$ ions have to be bonded to $Ca^{2+}$ ions, so the compound given by **4** must be considered to be a special mixture of